

# Comparative Evaluation of Texture Analysis Algorithms for Defect Inspection of Textile Products<sup>1</sup>

S. Özdemir<sup>1</sup>, A. Baykut<sup>2</sup>, R. Meylani<sup>3</sup>, A. Erçil<sup>2</sup> and A. Ertüzün<sup>3</sup>

<sup>1</sup>Computer Engineering, <sup>2</sup>Industrial Engineering, <sup>3</sup>Electrical and Electronic Engineering  
Boğaziçi University, Bebek, İstanbul, Turkey 80815  
[ercil@boun.edu.tr](mailto:ercil@boun.edu.tr) [ertuz@boun.edu.tr](mailto:ertuz@boun.edu.tr)

## Abstract

*Quality control is one of the basic issues in textile industry. Texture analysis plays an important role in the automated visual inspection of texture images to detect their defects. For this purpose, model-based and feature-based methods are implemented and tested for textile images in a laboratory environment. The methods are compared in terms of their success rates in determining the defects.*

## 1. Introduction

Quality inspection of textile products is an important problem for fabric manufacturers. Currently, the quality control of a fabric of width 1.6-2.0m. which moves at a speed of 8-20 m/min is mostly done by human operators.

Texture analysis plays an important role in automatic visual inspection of surfaces. There has been a limited number of applications of texture processing techniques to automated inspection problems[1-4]. For recent surveys of texture analysis, see [8-9].

In this paper, Markov random fields, Karhunen-Loève Transform, 2-D Lattice Filters, Laws Filters, the Co-occurrence method and the FFT-based method are implemented and are tested on real fabric images.

## 2. Evaluation of Texture Analysis Algorithms on Textile Images

The experiments are carried out on 256x256 gray level images taken by a Sony CCD Iris SSC-M370CE camera in a laboratory environment. The images were taken to have a resolution of 3.33 pixels/mm which is the same resolution that is required in the factory environment. Effort was made to include various textures and different

types of defects. The procedure that was carried out in the laboratory is as follows: The original 256x256 images are subdivided into non-overlapping 32x32 sub-windows. For each sub-window, the appropriate feature vectors are found and then the Mahalanobis distances for the feature vectors are computed. A sub-window is declared to be defective if its Mahalanobis distance lies outside the admissible range which is defined to be the region  $n$  quartiles from the median, where  $n$  is an experimental parameter. The results are summarized in Table I and are explained in the following subsections.

Each subsection of the table corresponds to the defective image given on the right-hand side of the table. The true number of defective sub-windows are noted at the bottom of the image. Columns 2, 5 and 8 of the table give the number of defective sub-windows found by the corresponding methods for the specified value of  $n$ . Columns 3, 6 and 9 give the number of sub-windows with false alarms. Columns 4, 7 and 10 give the percentage of the sub-windows that are correctly classified.

### 2.1 Markov-Random Field Models

For the Markov Random Field models, the sufficient statistics of each sub-window are used as the feature vector[1,2]. To model the texture, 5<sup>th</sup>, 9<sup>th</sup> and 14<sup>th</sup> order Markov Random Field models are used which are denoted by mrf 5, mrf 9 and mrf 14, respectively.

As seen in Table I, the performance of the 9<sup>th</sup> and 14<sup>th</sup> orders of the MRF methods are almost the same and better than the 5<sup>th</sup> order. In this case, the 9<sup>th</sup> order with less features could be chosen for efficiency purposes. As expected, the performance locating the defects and the number of false alarms increases as the  $n$  parameter decreases.

---

<sup>1</sup> This work has been partially supported by Turkish Technology Development Foundation under contract number TTGV-169. The fabrics were provided by Altunyıldız A.Ş..

## 2.2 Karhunen-Loève transform

The features in this case are the features derived from the eigenvalues of the covariance matrix of each sub-window:

eigenval5: The largest 5 eigenvalues.

eigenval7: The largest 7 eigenvalues. (7 values per sub-window)

eigenval9: The largest 9 eigenvalues.

normdiff5: The first 5 normalized differences (differences of the largest 5 eigenvalues taken and normalized with respect to the median eigenvalue)

normdiff7: The first 7 normalized differences

value3su: The sum of the 3 largest eigenvalues

value5su: The sum of the 5 largest eigenvalues

As can be seen from Table I, number of false alarms decline steeply as the admissible range is widened. The number of defective windows detected shows a similar behavior, but, at a lower rate. Among the Karhunen-Loève Transform based methods, eigenval5 seems to give a noticeably better performance for  $n = 4$  and  $n = 3$ .

## 2.3 2-D lattice filters

In this case, each  $32 \times 32$  subwindow is used as the input to the 12-parameter 2-D lattice filter structure [5]. The features are the reflection coefficients of the first stage, calculated using the method of least squares. As seen in Table I, the performance of the Lattice Filter method is insensitive to the value of  $n$ ; hence, it is more robust.

## 2.4 Laws Filters

Each sub-window is convolved with nine different 2-D Laws filters to obtain filtered images. Then, the sum of the squares or absolute values of the nine filtered images are put in a vector to form the feature vector (nine elements/vector for each sub-window).

Laws Filters method exhibits a performance comparable to the Karhunen-Loève Transform based methods. It can be seen that the performance of the laws method is slightly better than that of the lawsa method for a high increase in computational cost.

## 2.5 Co-occurrence method

In the co-occurrence method, the original image is first histogram-equalized and quantized to 8 gray levels. Then, the spatial-dependence matrices are formed for  $d = 1$  and  $0^\circ, 45^\circ, 90^\circ$  and  $135^\circ$ . From these matrices, four features (angular second moment, contrast, correlation and entropy) are computed to obtain the elements of the feature vector. The performance of the co-occurrence method is one of the worst with respect to all the criteria. This may be due to the high noise in the images, which makes modeling the probability distribution process error-prone.

## 2.6 FFT-based method

In the FFT-based method, first the Fast Fourier Transform of each sub-window is taken. Then, each  $32 \times 32$  sub-window is further divided into  $4 \times 4$  blocks whose energies are taken to be the elements of the feature vector for that sub-window.

As can be observed in Table I, the performance of the FFT-based method exhibits a pattern similar to the other methods. False alarm rate for this method is among the lowest of all the methods.

## 3. Summary and Conclusions

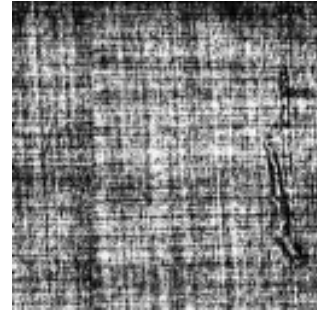
In this paper, various texture analysis methods have been studied for defect inspection of textile fabrics. For each method, the effects of various parameters have been examined. Although many of the methods gave promising results, texture modeling using the 9<sup>th</sup> order Markov Random Field model gave the best results. Considering the results obtained with respect to speed and the reliability, this approach seems feasible for a real-time factory implementation.

## References

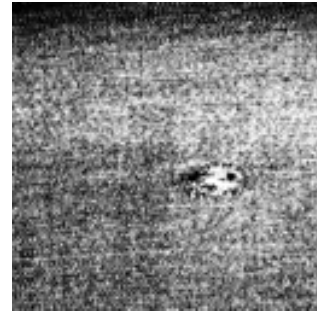
- [1] Atalay, A. "Automated Defect Inspection of Textile Fabrics Using Machine Vision Techniques", M.S. Thesis, Bogaziçi University, 1995.
- [2] Cohen, F., Fan, Z., Attali, S., "Automated Inspection of Textile Fabrics Using Textural Models," *IEEE PAMI*, V. 13, No. 8, August 1991.
- [3] Conners, R. et.al. "Identifying and locating surface defects in wood" *IEEE PAMI*, V. 5, No. 6, Nov. 1983.
- [4] Erçil, A., Özüyılmaz, B., "Automated Visual Inspection of Metallic Surfaces," *Proceedings ICARCV'94*, pp. 1950-1954, Singapore, Nov. 1994.
- [5] French, P.A., Zeidler, Z.A. and Ku, W.H. "Enhanced Detectability of Small Objects in Correlated Clutter Using an Improved 2-D Adaptive Lattice Algorithm", *IEEE Trans. On Image Proc.* Dec. 1996.
- [6] Laws, K.I., Textured Image Segmentation, Report 940, Image Processing Institute, University of Southern California.
- [7] Meylani, R., Ertüzün, A., Erçil, A., "A Comparative Study on the Adaptive Lattice Structures in the Context of Texture Defect Detection", *Proceedings of ICECS 96*, Vol.2, p.976-979, October 13-16, 1996, Greece.
- [8] Tuceryan, M., Jain, A., "Texture Analysis," *The Handbook of Pattern Recognition and Computer Vision*, by C.H. Chen, L.F. Pau, P.S.P. Wang (eds.) World Scientific Publishing Co., 1993.
- [9] Van Gool, L., P. Dewaele, and A. Oosterlinck "Survey: texture analysis anno 1983." *Computer Vision, Graphics, and Image Processing*, Vol. 29, p. 336-357. (1985)

Method	n=4-T	n=4-F	n=4-%	n=3-T	n=3-F	n=3-%	n=2-T	n=2-F	n=2-%
co-occur	3	2	87.5	3	4	84.4	4	1	75.0
lawsa	1	2	84.4	2	7	78.1	4	13	71.9
lawss	2	1	87.5	2	3	84.4	2	7	78.1
mrf 5	4	0	92.2	6	1	93.8	6	2	92.2
mrf 9	5	0	93.8	6	0	95.3	7	1	95.3
mrf 14	4	0	92.2	4	0	92.2	6	0	95.3
normdiff5	2	2	85.9	2	4	82.8	2	6	79.7
normdiff7	2	1	87.5	2	3	84.4	2	9	75.0
eigenval5	3	3	85.9	4	3	87.5	5	8	81.2
eigenval7	3	1	89.1	5	3	89.1	5	7	82.8
eigenval9	2	0	89.1	3	2	87.5	5	5	85.9
evaluate3su	4	1	90.6	4	2	89.1	4	4	85.9
evaluate5su	4	1	90.6	4	3	87.5	4	5	84.4
lattice	2	6	79.7	3	7	79.7	3	7	79.7
ffitbased	1	0	87.5	1	1	85.9	4	4	85.9
co-occur	2	2	96.9	2	2	96.9	2	7	89.1
lawsa	1	2	95.3	1	3	93.8	1	12	79.7
lawss	1	0	98.4	2	3	95.3	2	11	82.8
mrf 5	2	1	98.4	2	1	98.4	2	1	98.4
mrf 9	2	0	100.0	2	1	98.4	2	5	92.2
mrf 14	2	0	100.0	2	0	100.0	2	0	100.0
normdiff5	1	3	93.8	1	3	93.8	2	12	81.2
normdiff7	1	3	93.8	1	4	92.2	1	6	89.1
eigenval5	1	1	96.9	1	1	96.9	2	6	90.6
eigenval7	1	3	93.8	2	4	93.8	2	11	82.8
eigenval9	1	2	95.3	1	2	95.3	2	12	81.2
evaluate3su	2	5	92.2	2	6	90.6	2	8	87.5
evaluate5su	2	4	93.8	2	6	90.6	2	7	89.1
lattice	1	3	93.8	1	3	93.8	1	3	93.8
ffitbased	2	0	100.0	2	2	96.9	2	15	76.6
co-occur	0	1	95.3	1	1	96.9	1	1	82.8
lawsa	1	1	96.9	1	5	90.6	1	13	78.1
lawss	0	0	96.9	1	1	96.9	1	5	90.6
mrf 5	1	2	95.3	1	2	95.3	1	4	92.2
mrf 9	1	1	96.9	1	1	96.9	1	3	93.8
mrf 14	1	0	98.4	1	1	96.9	1	2	95.3
normdiff5	1	3	93.8	2	4	93.8	2	12	81.2
normdiff7	1	2	95.3	2	3	95.3	2	8	87.5
eigenval5	2	2	96.9	2	2	96.9	2	12	81.2
eigenval7	1	2	95.3	2	2	96.9	2	4	93.8
eigenval9	1	1	96.9	2	2	96.9	2	6	90.6
evaluate3su	2	1	98.4	2	3	95.3	2	8	87.5
evaluate5su	1	1	96.9	1	3	93.8	2	7	89.1
lattice	0	5	89.1	0	6	87.5	0	6	87.5
ffitbased	1	0	98.4	1	1	96.9	1	5	90.5
co-occur	1	0	89.1	1	3	84.4	2	1	70.3
lawsa	3	2	89.1	4	2	90.6	5	4	89.1
lawss	1	1	87.5	2	3	85.9	3	9	78.1
mrf 5	1	0	89.1	3	0	92.2	3	1	90.6
mrf 9	2	0	90.6	3	0	92.2	4	0	93.8
mrf 14	1	0	89.1	2	0	90.6	3	2	89.1
normdiff5	0	4	81.2	1	7	78.1	3	14	70.3
normdiff7	0	1	85.9	0	3	82.8	2	9	76.6
eigenval5	1	1	87.5	1	3	84.4	2	11	73.4
eigenval7	0	1	85.9	0	1	85.9	2	6	81.2
eigenval9	0	1	85.9	0	2	84.4	1	10	73.4
evaluate3su	0	3	82.8	1	4	82.8	1	6	79.7
evaluate5su	0	3	82.8	1	4	82.8	1	6	79.7
lattice	2	4	84.4	3	4	85.9	3	4	85.9
ffitbased	1	0	89.1	3	0	92.2	4	5	85.9
co-occur	1	1	87.5	1	5	81.2	1	1	68.8
lawsa	3	1	90.6	3	1	90.6	4	14	71.9
lawss	2	1	89.1	4	4	87.5	4	8	81.2
mrf 5	3	0	95.3	3	0	95.3	5	2	95.3
mrf 9	3	0	95.3	6	0	100.0	6	0	100.0
mrf 14	5	0	98.4	5	0	98.4	5	2	95.3
normdiff5	1	5	81.2	1	7	78.1	1	12	70.3
normdiff7	1	3	84.4	1	6	79.7	2	16	65.6
eigenval5	2	3	85.9	2	4	84.4	3	11	75.0
eigenval7	1	2	85.9	2	2	87.5	2	9	76.6
eigenval9	1	0	89.1	1	2	85.9	2	9	76.6
evaluate3su	1	2	85.9	1	4	82.8	3	6	82.8
evaluate5su	1	5	81.2	2	6	81.2	3	8	79.7
lattice	4	9	82.8	4	9	82.8	4	10	81.3
ffitbased	0	0	87.5	0	1	85.9	1	8	76.6

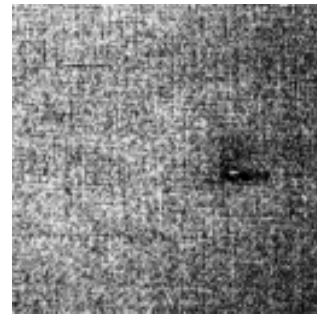
Table.I Summary of Experimental Results



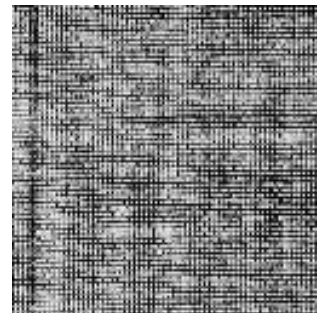
9 Defective Sub-windows



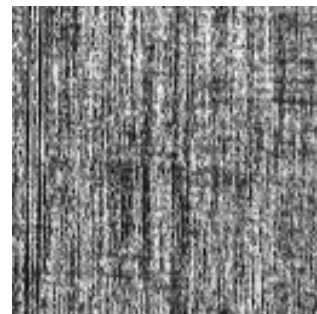
2 Defective Sub-windows



2 Defective Sub-windows



8 Defective Sub-windows



6 Defective Sub-window